Ultraviolet B irradiation-induced keratinocyte senescence and impaired development of 3D epidermal reconstruct

SUVARA K. WATTANAPITAYAKUL[1,*]
LINDA CHULAROJMONTRI[2]
MONIKA SCHÄFER-KORTING[3]

[1] *Department of Pharmacology*
Faculty of Medicine, Srinakharinwirot
University, Bangkok 10110, Thailand

[2] *Department of Preclinical Sciences*
Faculty of Medicine, Thammasat
University, Klongluang, Pathumthani
12120, Thailand

[3] *Institute for Pharmacy, Freie*
Universität Berlin, 14195 Berlin
Germany

Ultraviolet B (UVB) induces morphological and functional changes of the skin. This study investigated the effect of UVB on keratinocyte senescence and the development of reconstructed human epidermis (RHE). Primary normal human keratinocytes (NHK) from juvenile foreskin were irradiated with UVB (30 mJ cm^{-2}) and these effects were compared to NHK that underwent senescence in the late passage. UVB enhanced the accumulation of reactive oxygen species (ROS) and halted cell replication as detected by BrdU cell proliferation assay. The senescence phenotype was evaluated by beta-galactosidase (β-gal) staining and qPCR of genes related to senescent regulation, *i.e.* p16INK4a, cyclin D2, and IFI27. Senescence induced by high dose UVB resulted in morphological changes, enhanced β-gal activity, elevated cellular ROS levels and reduced DNA synthesis. qPCR revealed differential expression of the genes regulated senescence. p16INK4a expression was significantly increased in NHK exposed to UVB whereas enhanced IFI27 expression was observed only in cultural senescence. The levels of cyclin D2 expression were not significantly altered either by UVB or long culturing conditions. UVB significantly induced the aging phenotype in keratinocytes and impaired epidermal development. RHE generated from UVB-irradiated keratinocytes showed a thinner cross-sectional structure and the majority of keratinocytes in the lower epidermis were degenerated. The 3D epidermis model is useful in studying the skin aging process.

Keywords: epidermis, keratinocytes, ultraviolet radiation, skin aging, senescence, reactive oxygen species

Skin aging is associated with intrinsic (genetically driven) and extrinsic factors such as accumulation of reactive oxygen species (ROS) and ultraviolet (UV) ray exposure. While UVC light (< 280 nm) is strongly absorbed by the atmosphere, UVA (320–400 nm) and UVB (280–320 nm) contribute to skin aging as well as the development of skin cancer. UVB induces the accumulation of senescent skin cells leading to morphological and physiological

* Correspondence; e-mail: suvara@gmail.com

changes that contribute to functional impairment. The causative molecular mechanisms involve many signaling pathways, including ROS stress, activation of the mechanistic target of rapamycin (mTOR), senescence-associated secretory phenotype (SASP), and resistance to apoptosis (1).

Increased ROS accumulation is detected during the aging process and correlates well with the aged phenotype. For example, the accumulation of hydrogen peroxide by mitochondria can be used as a marker of aging (2). Optimal ROS levels and redox homeostasis support normal physiological functions of the cells while oxidative stress can trigger molecular mechanisms controlling the onset of senescence through damaging the cell's DNA, respiratory chain, membranes and proteins (3). In responses to alterations in redox balance, ROS arises from UVB irradiation can influence transcription factors such as p53, Nrf2, and cell cycle-regulated proteins such as cyclins, cyclin-dependent kinases (CDKs), as well as a common marker for cellular senescence and aging, the tumor suppressor protein p16INK4a (4, 5). These cellular adaptation pathways thrive cells on apoptosis resistance and senescent phenotypic alterations. Therefore, changes in gene expression can be used as markers for studying UVB-induced senescence as well as cells that underwent cultural senescence.

Apart from cell culture studies, the development of the 3D skin aging model can facilitate aging studies in the dermatological research field. Reconstructed human epidermis (RHE) and reconstructed human full-thickness skin (RHS) consisting of cells isolated from juvenile foreskin and further cultured in multi-layers that resemble normal human epidermis and human skin, respectively. These reflect morphology and function of the human tissue which are suitable for testing chemical compounds for local toxicity including nanomaterials (6, 7) as well as testing for percutaneous absorption (8), and local metabolism (9). However, with respect to research on aging, the use of those models is at its early stage (10). Here we extend the insight into the induction of keratinocyte senescence by UVB irradiation and describe the construction of RHE reflecting skin aging.

<div align="center">EXPERIMENTAL</div>

Materials

If not indicated otherwise, all chemicals used in this study were purchased from Sigma--Aldrich Chemie GmbH (Germany). The purity of the chemicals is Reagent Grade for general buffer preparations and Cell Culture Grade for used in cell culture experiments.

Isolation and cultivation of human keratinocytes

Normal human keratinocytes (NHK) from the juvenile foreskin, leftovers of clinically indicated surgery (ethical approval EA1/081/13). The parents of foreskin donors had signed the written informed consent for scientific use. NHK were isolated and expanded in Corning cell culture ware (USA) as described (10). The pooled of NHK from two to three samples were grown in Keratinocyte Basal Medium with supplements (KGM™ BulletKit™, procured from Lonza, Switzerland) at 37 °C and 5 % CO_2 for up to 3 passages, if not indicated otherwise.

UVB irradiation

NHK up to passage 5 were cultured in 100-mm dish until reaching 80 % confluences were washed with phosphate-buffered saline (PBS) and overlaid with PBS 2 mL before exposure to UVB at 30 mJ cm^{-2} (Bio-Link®, Vilber Lourmat, Germany). The UVB dose was selected based on the dose-response curve and the lower limit of the UV equipment. The UVB source delivered the peak spectrum at 312 nm and energy at the rate of 4.28 mJ s^{-1}. After UVB irradiation, the medium was changed and cells were incubated for 24 h. Non-irradiated (sham) cells served for control experiments (CTRL).

Effect of UVB on cell viability

NHK (5 × 10^5 cells per well) were grown in 96-well plate prior to UVB exposure at various UVB doses (30 to 90 mJ cm^{-2}). First, cells were washed twice with cold PBS and overlaid with 20 μL cold PBS while exposed to UVB. Then cells were further cultured for 24 h and the yellow tetrazolium MTT (final concentration of 0.5 mg mL^{-1}) was added to each well for additional 3-h incubation. After the supernatant was discarded, 100 μL of DMSO was added to each well to dissolve the purple formazan complex derived from MTT mitochondrial metabolism. The samples were read at the absorbance of 540 nm. Cell viability was calculated relative to the non-UV exposed cells (CTRL, 100 % cell viability).

Cell proliferation assay

NHK (5 × 10^4 cells per well), seeded into a 96-well plate, were subjected to UVB irradiation (30 mJ cm^{-2}) or 5-fluorouracil (5-FU) application. After 24 h bromodeoxyuridine (BrdU) incorporation was evaluated (BrdU cell proliferation assay kit, Calbiochem, USA), following the manufacturer's instructions.

Senescence-associated β-galactosidase activity (SA-β-gal)

Seventy-two hours after UVB exposure, 5 × 10^4 cells grown in a 6-well plate were β-gal stained using a histochemical staining kit (Sigma-Aldrich, Germany) according to the manufacturer's instruction. Sham cells served for control. Briefly, following fixation with fixation buffer for 10 min at room temperature and washing with PBS 3 times, cells were incubated with the staining mixture 1 mL per well for 24 h at 37 °C (without CO$_2$). Blue stained cells were counted under an inverted microscope.

ROS levels measured by flow cytometry

NHK (5 × 10^5 and 5 × 10^6 cells) were collected by trypsinization, washed once with PBS, and resuspended in 500 μL of PBS containing 0.5 % bovine serum albumin (BSA) and 2 mM EDTA. Following excitation at 480 nm, ROS related cellular autofluorescence was recorded using a 530/30 bandpass filter (Beckman Coulter Cytoflex, USA). The amounts of ROS were represented as the mean values of cell population autofluorescence.

Reverse transcription-polymerase chain reactions (RT-PCR)

Total RNA was extracted from cultured NHK using the NucleoSpin RNA II kit (Macherey-Nagel, Germany). After the removal of remnant DNA by DNAase I (Sigma-

-Aldrich), 1 μg of RNA was converted to cDNA by RevertAid First Strand cDNA Synthesis Kit (ThermoFisher Scientific, USA) performing 45 cycles with denaturation step at 94 °C, 10 s followed by annealing at 60 °C, 10 s, and extension at 72 °C for 10 s. Amplification was terminated with a 10-min extension at 72 °C. Relative mRNA amounts of samples were calculated using the comparative CT method (ΔΔCt method) with reference to the standard curve (Lightcycler 480, Roche). Primers for PCR amplification of housekeeping genes and specific genes were used as described previously, *i.e.*, p16INK4a, Cyclin D2, IFI27, and SDHA (4, 11, 12).

RHE reconstruction

The human epidermis was reconstructed using NHK at passage 3. RHE-UVB was built from UVB-irradiated (30 mJ cm^{-2}) cells while RHE from non-irradiated NHK served for control. 2×10^5 cells seeded onto polycarbonate membrane inserts (Millicell®-PCF, 0.4 μm, Millipore Sigma, USA) were allowed to grow in 400 μL KGM for 2 to 3 days. To assure that cells have grown to confluences in the inserts, we did the examination by light microscopy followed by the CnT-ST staining (CellNTech, Switzerland) which indicated homogenous blue staining of the bottom surface of the representative insert. Next, cells in the insert were covered with 3D Prime Differentiation Medium (CELLnTEC, Switzerland) to induce the formation of intercellular adhesion structures (CO_2/37 °C). The next day 3D growth was initiated by the airlift of the culture, media was changed every other day for 14 days. Morphology study was derived by light microscopy from RHE embedded in OCT (Tissue-Tec® Cryomold®, VWR, PA, USA), cryo-sectioned at –20 °C (Leica CM 1510S) into 5 μm slices and stained with hematoxylin and eosin (H&E).

Statistical analysis

All measurements were performed in triplicate and $n = 3$ (pooled cells of 2–3 donors for each n), results are expressed as means ± standard error of the mean (SEM). The data sets were compared and analyzed using *t*-test or one-way analysis of variance (ANOVA) with Newman-Keuls posthoc test. $p < 0.05$ is considered statistically significant.

RESULTS AND DISCUSSION

UVB reduces cell viability and proliferation

As shown in Fig. 1a, UVB dose-dependently decreased cell survival starting at 30 mJ cm^{-2} (lower limit of UV machine). NHK undergone senescence markedly showed a reduction in cell proliferation as demonstrated by the incorporation of BrdU during DNA synthesis. NHK exposed to UVB demonstrated a reduction of BrdU incorporation by 47.7 ± 4.7 % *vs.* control. This is close to the effect induced by the anti-metabolite 5-FU at 10 μM (Fig. 1b). The mechanisms of UVB-induced apoptosis associated with increased p53 and degradation of cyclin-dependent kinase (CDK) inhibitor p21, resulted in dysregulation of cell cycle arrest and DNA repair process (13). Additionally, mTOR signaling in UVB-induced apoptotic cells may be suppressed leading to inactivations of the autophagy, proliferation, and AKT cell survival pathways (14).
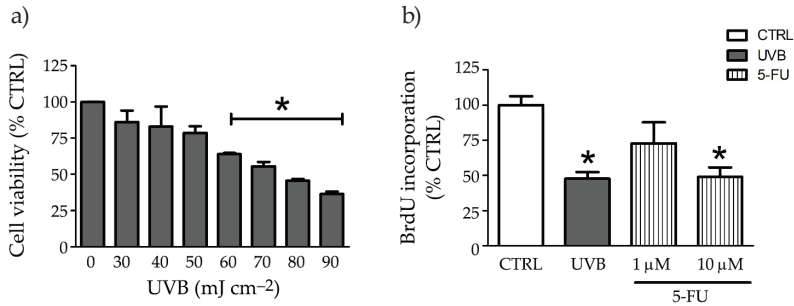
Fig. 1. Effects of UVB on NHK cell survival and proliferation. a) Relationship of UVB dose and NHK cell viability. NHK were exposed to UVB at different doses as indicated in the figure. Cell viability was evaluated by MTT assay using non-UV NHK as a control CTRL, 100 % cell viability); b) UVB and 5-FU exposure inhibited NHK proliferation. NHK at passage 3 were irradiated with UVB at 30 mJ cm^{-2} and BrdU incorporation was quantified after 24 h as described in Materials and Methods. 5-FU was used as positive controls; * $p < 0.05$ *vs.* negative control (CTRL).

Keratinocyte senescence induced by UVB exposure and extended subcultivation

Primary NHK at the early passage as passage 3 (p3) formed polygonal cell monolayer (Fig. 2a) whereas cells at high passages depicted larger size and irregular shape (Fig. 2c). Keratinocytes reached senescence at passage 5 (p5) characterized by SA-β-gal staining had approximately 4-fold increase versus passage 3 (4.48 ± 0.30 % *vs.* 17.65 ± 0.67 %, respectively;
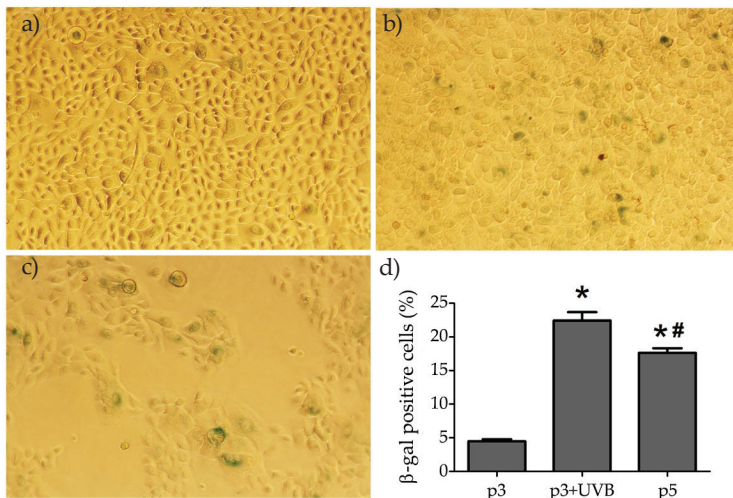

Fig. 2. Morphology of keratinocytes and the staining of beta-galactosidase (β-gal). a) Representative photos of NHK were taken at passage 3 (p3) without UVB exposure and b) p3 with UVB exposure at 30 mJ cm^{-2}; c) NHK underwent normal culture to passage 5 (p5); d) calculated percent β-gal positive NHK. * $p < 0.05$ *vs.* non-UVB p3; #, $p < 0.05$ *vs.* p3+UVB. Photos were captured at 100× magnification.

Fig. 2d) while UVB (30 mJ cm^{-2}) irradiation to NHK at p3 induced the senescent phenotype but the extent of SA-β-gal staining was higher as compared to cells at passage 5 (5-fold increase to 22.43 ± 1.26 % (Fig. 2b,c). NHK in this experiment rapidly reached replicative senese due to the high calcium concentration (more than 0.1 mmol L^{-1}) of the growth medium which induced the cease of cell proliferation earlier than the cultures grown under low calcium medium (less than 0.1 mmol L^{-1}) (15, 16). Thus, the control of calcium levels is crucial for triggering cell division or stress-induced senescence.

Intracellular ROS levels

Senescence became obvious from an alteration in ROS related autofluorescence at 480/530 nm. The effect seen in NHK at late passages was not different from the younger passage at p3 while NHK irradiated with UVB showed a significant increase in ROS up to 172.26 ± 24.54 % when compared to non-irradiated cells (Fig. 3a,b). Intracellular ROS accumulation is another key phenomenon found both in NHK undergone replicative aging as well as premature aging induced by UVB. Superoxide anion, hydrogen peroxide, hydroxyl radical, and peroxynitrite are the major ROS produced during UV irradiation in keratinocytes (19). These ROS induced oxidative stress (ROS/p38 MAPKs pathways), DNA damage, and inflammation (COX-2 and PGE2 production) (20, 21). Thus, using antioxidants can reduce the detrimental effects of UVB-induced oxidative damage to the keratinocytes (22).

Senescence-related gene expression

The mRNA expression of genes associated with aging was evaluated by qPCR. While cyclin D2 was unaltered following UVB irradiation as well as in non-irradiated NHK at
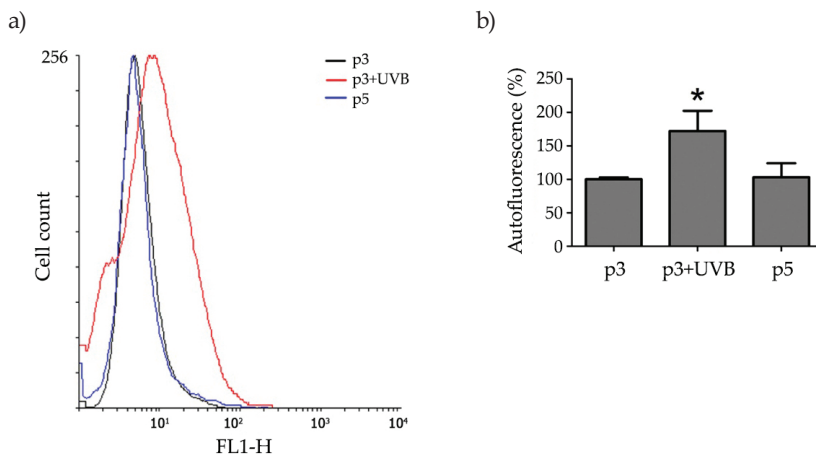

Fig. 3. Flow cytometry analysis of autofluorescence in keratinocytes. The X-axis is autofluorescence detected at 480/530 nm and the Y-axis is the cell count as described in Materials and Methods. a) The autofluorescence of NHK at different cell conditions, *i.e.*, passage 3 (p3), p3 irradiated with UVB 30 mJ cm^{-2} (p3+UVB), and NHK at passage 5 (p5); b) The bar graph represents the percentage of autofluorescent cells. * $p < 0.05$ when compared with p3 (non-UVB).
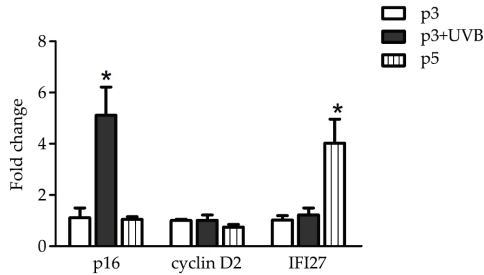
Fig. 4. Fold changes in gene expression by extended subcultivation of keratinocytes passage 5 (p5) *vs.* passage 3 (p3) and those induced by UVB (30 mJ cm^{-2}) irradiation. Gene expression including p16INK4a, cyclin D2, and IFI27 was detected by RT-PCR. p = passage; UVB = NHK undergone UVB irradiation. Native expression of p3 was set at 1. * $p < 0.05$ indicates changes related to p3.

passage 5, differential effects were seen in genes encoding IFI27 and p16INK4a. Elevations of IFI27 (4.0 ± 0.9 folds) were found in NHK at passage 5 and elevations of p16INK4a (5.1 ± 0.1 folds) in NHK passage 3 following UVB irradiation, respectively (Fig. 4).

The intrinsic and extrinsic inducers for aging share similar signals, yet certain differences in pathways of activation are also observed. The common outcomes of oxidative processes in the aging skin include mitochondrial dysfunction, redox signaling alteration, genome instability, and cellular senescence. Three genes involved in different aspects of cellular aging and UVB exposure were selected for comparison, *i.e.*, p16INK4a, cyclin D2, and IFI27. Among these, the overexpression of p16INK4a is commonly observed in skin aging while cyclin D2 and IFI27 are more ligand- and pathophysiology-specific responses (23, 24). In this study, UVB markedly induced p16INK4a expression in NHK while this phenomenon was not observed in cells that underwent culturing senescence. Elevation of p16INK4a expression was also observed in the basal layer of a human skin equivalent but not cyclin D2, a regulator of Cdk4/6 for the G1/S phase transition, which remained unchanged in both conditions (cell culture and RHE) (23). This suggests that the regulation of cyclin-dependent kinase inhibitors (CKIs), such as p16INK4a, is more prominent as a marker of differential status of senescence features.

Another change in the gene expression observed in this study was IFI27, a regulator of cell proliferation, cell cycle, and immune system. IFI27 is involved in upregulated in certain inflammatory skin diseases and conditions, including psoriasis, cutaneous squamous cell cancers, and wound repair (25). Significant elevation of IF27 expression was observed only in NHK passage 5 but found only a minimal change in young NHK irradiated with UVB. Microarray analysis of different human skin ages reveals that expression of IFI27 was among the 198 genes that peculiar to aged skin (26). It is possible that intrinsic senescence and photoaging acquire diverse regulators (27) and the changes of IFI27 may have an implication as a marker for skin aging. Additionally, activation of the inflammatory process, as well as aging-related proteins, were observed in human immortal keratinocytes, HaCaT cells, irradiated with UVB (28). Enhanced MMP-1 and proinflammatory cytokines (IL-1β and IL-6) production but decreased silent information regulator T1 (SIRT1) signaling were suggested as participants in the photoaging process.

Histological appearance of 3D keratinocyte epidermal reconstructs

The 3D reconstruction of the epidermis model was established within 14 days of culture. The histological structure revealed that the 3D construct composed of 5–6 layers of keratinocytes that stratified from the bottom layer closed to the artificial membrane of the insert to form stratum corneum on the uppermost layers (Fig. 5a). On the contrary, the 3D epidermis model generated from KCs that underwent UVB irradiation (30 mJ cm^{-2}) showed a thinner cross-sectional structure and most cells were degenerated or differentiated (Fig. 5b). A thick layer of stratum corneum was observed (approximately 30 % of the dermis) in the model using normal KCs at passage 3 whereas markedly thinner stratum corneum was developed in the model constructed from UVB irradiated KCs.

Not only were UVB-induced changes detected in the keratinocyte monolayer culture but modifications were observed in 3D epidermal morphology. Built from differentiating keratinocytes, RHE is a well reflecting upper layer of human skin. Only this model can be used for the evaluation of drug absorption (8), and it is superior to the monolayer cell culture when studying metabolism and toxicity (29). Additionally, the 7th Amendment to the Cosmetics Directive of the European Union prohibits animal testing of cosmetics in full; therefore, for effective substances, *in vitro* models are required to fulfill the needs of safety testing. A 3D *in vitro* epidermis model generated from human cells is needed for risk analysis in the aging population. This study shows that using UVB-induced senescent keratinocytes for tissue reconstruction impaired the development and maturation of human epidermis. UVB-exposed NHK could partially develop the stratum corneum but the granular, spinosum and basal layers were dramatically deformed. It is possible that the senescent UVB-irradiated NHK had reduced ability to proliferate (no granular layer) whereas final differentiation (stratum corneum) appears relatively less affected. The family of INK4 proteins has a specific function in blocking cyclin D-CDK4/6 activity that quarantines the cells to G1 phase arrest (30). It is possible that NHK exposed to UVB had raised INK4a and prohibited cell proliferation. Additionally, p53 may also involve in controlling the expression
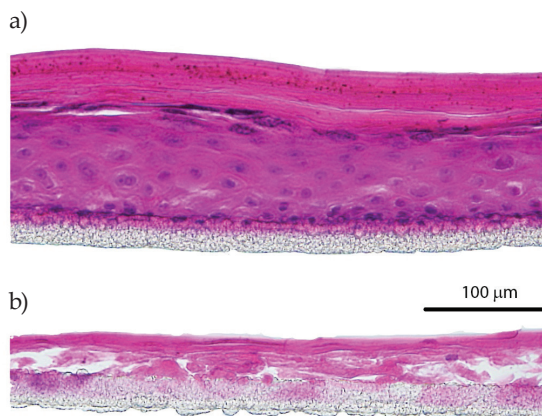

Fig. 5. Hematoxylin-Eosin staining of RHE. a) Epidermis cultured from keratinocytes at passage 3; b) Epidermis cultured from KC passage 3 irradiated with UVB at 30 mJ cm^{-2}.

of p21/Cip1 which in turn, may lead to the inhibition of cyclin-CDK4/6 activity. The induction of photoaging by UV engages at least three important pathways (31). First, UV activates the AP1 complex that further causing collagen breakdown through the MMP-1 and MMP-9 signals. Second, UV suppresses TGF-β function which, in normal condition, activates Smad2, procollagen synthesis. Finally, UV suppresses PI3K/Akt/mTOR signaling and autophagy pathway (32).

The understanding of functional and molecular regulation of dermal keratinocyte aging is crucial for defining strategies that are appropriate for skin care and skin disease therapy in the aging population. The changes in epidermal morphology even following the lower UV doses resulted in an impaired barrier function and allow nanoparticles (molecular mass about 80.000 Da) to pass the stratum corneum and access viable epidermis (10). More studies are warranted for reconstructing full-thickness skin in the light of skin aging, particularly skin repair and protection of photoaging.

CONCLUSIONS

UVB significantly induced the aging phenotype in keratinocytes and impaired epidermal development. RHE generated from UVB irradiated keratinocytes showed a thinner cross-sectional structure whereas the majority of keratinocytes in the viable epidermis layer were degenerated. The 3D epidermis model improves the understanding of skin aging. We believe that this model of UVB-induced impairment of epidermal development could help with a better understanding of the molecular changes and design of therapeutic strategies for the skin disease related to UVB or for the prevention of skin aging. This also in concordance with the reduction of animal use and the policy of prohibitions testing cosmetics on animals in the EU.

REFERENCES

1. R. Sharma and Y. Padwad, In search of nutritional anti-aging targets: TOR inhibitors, SASP modulators, and BCL-2 family suppressors, *Nutrition* **65** (2019) 33–38; https://doi.org/10.1016/j.nut.2019.01.020

2. T. Zuliani, V. Denis, E. Noblesse, S. Schnebert, P. Andre, M. Dumas and M. H. Ratinaud, Hydrogen peroxide-induced cell death in normal human keratinocytes is differentiation dependent, *Free Radic. Biol. Med.* **38** (2005) 307–316; https://doi.org/10.1016/j.freeradbiomed.2004.09.021

3. P. Davalli, T. Mitic, A. Caporali, A. Lauriola and D. D'Arca, ROS, cell senescence, and novel molecular mechanisms in aging and age-related diseases, *Oxid. Med. Cell. Long.* **2016** (2016) 3565127; https://doi.org/10.1155/2016/3565127

4. B. W. Darbro, G. B. Schneider and A. J. Klingelhutz, Co-regulation of p16INK4A and migratory genes in culture conditions that lead to premature senescence in human keratinocytes, *J. Invest. Dermatol.* **125** (2005) 499–509; https://doi.org/10.1111/j.0022-202X.2005.23844.x

5. M. Sasaki, H. Kajiya, S. Ozeki, K. Okabe and T. Ikebe, Reactive oxygen species promotes cellular senescence in normal human epidermal keratinocytes through epigenetic regulation of p16(INK4a.), *Biochem. Biophys. Res. Commun.* **452** (2014) 622–628; https://doi.org/10.1016/j.bbrc.2014.08.123

6. N. Alépée, M. H. Grandidier and J. Cotovio, Sub-categorisation of skin corrosive chemicals by the EpiSkin™ reconstructed human epidermis skin corrosion test method according to UN GHS: Revision of OECD Test Guideline 431, *Toxicol. In Vitro* **28** (2014) 131–145; https://doi.org/10.1016/j.tiv.2013.10.016

7. C. Gerecke, A. Edlich, M. Giulbudagian, F. Schumacher, N. Zhang, A. Said, G. Yealland, S. B. Lohan, F. Neumann, M. C. Meinke, N. Ma, M. Calderon, S. Hedtrich, M. Schafer-Korting and B. Kleuser, Biocompatibility and characterization of polyglycerol-based thermoresponsive nanogels designed as novel drug-delivery systems and their intracellular localization in keratinocytes, *Nanotoxicology* **11** (2017) 267–277; https://doi.org/10.1080/17435390.2017.1292371

8. M. Schafer-Korting, U. Bock, A. Gamer, A. Haberland, E. Haltner-Ukomadu, M. Kaca, H. Kamp, M. Kietzmann, H. C. Korting, H. U. Krachter, C. M. Lehr, M. Liebsch, A. Mehling, F. Netzlaff, F. Niedorf, M. K. Rubbelke, U. Schafer, E. Schmidt, S. Schreiber, K. R. Schroder, H. Spielmann and A. Vuia, Reconstructed human epidermis for skin absorption testing: results of the German pre-validation study, *Alternat. Lab. Animals* **34** (2006) 283–294.

9. F. M. Batz, W. Klipper, H. C. Korting, F. Henkler, R. Landsiedel, A. Luch, U. von Fritschen, G. Weindl and M. Schafer-Korting, Esterase activity in excised and reconstructed human skin-biotransformation of prednicarbate and the model dye fluorescein diacetate, *Eur. J. Pharm. Biopharm.* **84** (2013) 374–385; https://doi.org/10.1016/j.ejpb.2012.11.008

10. L. J. Lowenau, C. Zoschke, R. Brodwolf, P. Volz, C. Hausmann, S. Wattanapitayakul, A. Boreham, U. Alexiev and M. Schafer-Korting, Increased permeability of reconstructed human epidermis from UVB-irradiated keratinocytes, *Eur. J. Pharm. Biopharm.* **116** (2017) 149–154; https://doi.org/10.1016/j.ejpb.2016.12.017

11. R. J. Perera, S. Koo, C. F. Bennett, N. M. Dean, N. Gupta, J. Z. Qin and B. J. Nickoloff, Defining the transcriptome of accelerated and replicatively senescent keratinocytes reveals links to differentiation, interferon signaling, and Notch related pathways, *J. Cell. Biochem.* **98** (2006) 394–408; https://doi.org/10.1002/jcb.20785

12. J. Vandesompele, K. De Preter, F. Pattyn, B. Poppe, N. Van Roy, A. De Paepe and F. Speleman, Accurate normalization of real-time quantitative RT-PCR data by geometric averaging of multiple internal control genes, *Genome Biol.* **3** (2002) RESEARCH0034.

13. X. Lei, B. Liu, W. Han, M. Ming and Y. Y. He, UVB-Induced p21 degradation promotes apoptosis of human keratinocytes, *Photochem. Photobiol. Sci.* **9** (2010) 1640–1648; https://doi.org/10.1039/c0pp00244e

14. T. D. Carr, J. DiGiovanni, C. J. Lynch and L. M. Shantz, Inhibition of mTOR suppresses UVB-induced keratinocyte proliferation and survival, *Cancer Prev. Res.* **5** (2012) 1394–404; https://doi.org/10.1158/1940-6207.CAPR-12-0272-T

15. J. W. Littlefield, Escape from senescence in human keratinocyte cultures, *Exp. Gerontol.* **31** (1996) 29–32.

16. G. A. Rockwell, G. Johnson and A. Sibatani, In vitro senescence of human keratinocyte cultures, *Cell Struct. Funct.* **12** (1987) 539–548.

17. C. L. Tu, W. Chang and D. D. Bikle, The calcium-sensing receptor-dependent regulation of cell-cell adhesion and keratinocyte differentiation requires Rho and filamin A, *J. Invest. Dermatol.* **131** (2011) 1119–1128; https://doi.org/10.1038/jid.2010.414

18. Z. Xie, S. M. Chang, S. D. Pennypacker, E. Y. Liao and D. D. Bikle, Phosphatidylinositol-4-phosphate 5-kinase 1alpha mediates extracellular calcium-induced keratinocyte differentiation, *Mol. Biol. Cell* **20** (2009) 1695–704; https://doi.org/10.1091/mbc.E08-07-0756

19. A. Dhumrongvaraporn and P. Chanvorachote, Kinetics of ultraviolet B irradiation-mediated reactive oxygen species generation in human keratinocytes, *J. Cosmet. Sci.* **64** (2013) 207–217.

20. U. Wolfle, P. R. Esser, B. Simon-Haarhaus, S. F. Martin, J. Lademann and C. M. Schempp, UVB-induced DNA damage, generation of reactive oxygen species, and inflammation are effectively attenuated by the flavonoid luteolin in vitro and in vivo, *Free Radic. Biol. Med.* **50** (2011) 1081–1093; https://doi.org/10.1016/j.freeradbiomed.2011.01.027

21. E. Takai, M. Tsukimoto, H. Harada and S. Kojima, Involvement of P2Y6 receptor in p38 MAPK-mediated COX-2 expression in response to UVB irradiation of human keratinocytes, *Radiat. Res.* **175** (2011) 358–366; https://doi.org/10.1667/RR2375.1

22. X. Ren, Y. Shi, D. Zhao, M. Xu, X. Li, Y. Dang and X. Ye, Naringin protects ultraviolet B-induced skin damage by regulating p38 MAPK signal pathway, *J. Dermatol. Sci.* **82** (2016) 106–114; https://doi.org/10.1016/j.jdermsci.2015.12.008

23. J. Adamus, S. Aho, H. Meldrum, C. Bosko and J. M. Lee, p16INK4A influences the aging phenotype in the living skin equivalent, *J. Invest. Dermatol.* **134** (2014) 1131–1133; https://doi.org/10.1038/jid.2013.468

24. N. Kanda and S. Watanabe, 17beta-estradiol stimulates the growth of human keratinocytes by inducing cyclin D2 expression, *J. Invest. Dermatol.* **123** (2004) 319–328; https://doi.org/10.1111/j.0022-202X.2004.12645.x

25. S. Suomela, L. Cao, A. Bowcock and U. Saarialho-Kere, Interferon alpha-inducible protein 27 (IFI27) is upregulated in psoriatic skin and certain epithelial cancers, *J. Invest. Dermatol.* **122** (2004) 717–721; https://doi.org/10.1111/j.0022-202X.2004.22322.x

26. P. Sextius, C. Marionnet, C. Tacheau, F. X. Bon, P. Bastien, A. Mauviel, B. A. Bernard, F. Bernerd and L. Dubertret, Analysis of gene expression dynamics revealed delayed and abnormal epidermal repair process in aged compared to young skin, *Arch. Dermatol. Res.* **307** (2015) 351–364; https://doi.org/10.1007/s00403-015-1551-5

27. W. L. Hsieh, Y. H. Huang, T. M. Wang, Y. C. Ming, C. N. Tsai and J. H. Pang, IFI27, a novel epidermal growth factor-stabilized protein, is functionally involved in proliferation and cell cycling of human epidermal keratinocytes, *Cell Prolif.* **48** (2015) 187–197; https://doi.org/10.1111/cpr.12168

28. H. K. Kim, Protective effect of garlic on cellular senescence in UVB-exposed HaCaT human keratinocytes, *Nutrients* **8** (2016); https://doi.org/10.3390/nu8080464

29. W. T. Liao, J. H. Lu, C. H. Lee, C. E. Lan, J. G. Chang, C. Y. Chai and H. S. Yu, An interaction between arsenic-induced epigenetic modification and inflammatory promotion in a skin equivalent during arsenic carcinogenesis, *J. Invest. Dermatol.* **137** (2017) 187–196; https://doi.org/10.1016/j.jid.2016.08.017

30. G. P. Studzinski, E. Gocek and M. Danilenko, Chapter 84: *Vitamin D Effects on Differentiation and Cell Cycle*, in *Vitamin D*, 3rd ed (Eds. D. Feldman, J. W. Pike, J. S. Adams) Academic Press, San Diego 2011, pp. 1625–1656.

31. H. W. Chiu, C. H. Chen, Y. J. Chen and Y. H. Hsu, Far-infrared suppresses skin photoaging in ultraviolet B-exposed fibroblasts and hairless mice, *PloS One* **12** (2017) e0174042; https://doi.org/10.1371/journal.pone.0174042

32. J. Feng, Y. Liao, X. Xu, Q. Yi, L. He and L. Tang, hnRNP A1 promotes keratinocyte cell survival post UVB radiation through PI3K/Akt/mTOR pathway, *Expe. Cell Res.* **362** (2018) 394–399; https://doi.org/10.1016/j.yexcr.2017.12.002